The benefits of elastic FWI in resolving sub-chalk imaging in the Southern North Sea

J. Johal[1], M. Oleszuk[1], N. Masmoudi[1], A. Ratcliffe[1], P. Smith[1], M. Burbidge[1]

[1] CGG

Summary

Acoustic full-waveform inversion (FWI) is widely employed to produce high-resolution subsurface models, especially for the P-wave velocity. However, more complex geological challenges, such as shallow chalk and salt, generate strong impedance contrasts that exhibit elastic effects, causing acoustic approximations to struggle. In parts of the Southern North Sea, fast shallow chalk outcrops at the water bottom and Zechstein salt geometries sit above target intervals, both severely challenging velocity model building and imaging. This shallow-water case study uses short-offset, dual-azimuth, towed-streamer data where the near-surface geological environment and maximum acquired offset limit the diving-wave penetration. While this acquisition scenario impacts both acoustic and elastic FWI, we demonstrate how elastic FWI out-performs acoustic FWI in updating the shallow chalk and provides an improved model for further updates to the deeper Zechstein evaporate and carbonate units. The comparisons illustrate how acoustic FWI slows the velocity model through the chalk interval, contrary to the sonic well-log measurements. Conversely, the equivalent elastic FWI better captures the chalk velocities and shallow complexities. The 15 Hz elastic FWI update down to the target depth demonstrates improved imaging over the whole section, highlighting how elastic FWI can become a key technology to handle these extremely difficult environments.

The benefits of elastic FWI in resolving sub-chalk imaging in the Southern North Sea

Introduction

Full-waveform inversion (FWI) has become a common velocity model building tool used to generate high-resolution subsurface models. The technology was first introduced in the 1980s and in recent times has become the tool of choice to update the P-wave velocity (Vp). Furthermore, FWI has fuelled additional advancements in the field of seismic imaging, i.e. FWI Imaging (Zhang et al., 2020). FWI seeks to minimise the misfit between recorded and modelled data through iterative updates of subsurface parameters. Historically, acoustic approximations have been used to limit the cost of forward modelling and, in most marine environments, this has been employed to great effect. However, in geological settings where strong impedance contrasts are present, elastic effects must be considered in FWI to derive a reliable model update (Plessix and Krupovnickas, 2021; Masmoudi et al., 2022; Wu et al., 2022). At sharp interfaces, mode conversions between P- and S-waves occur which affect the phase and amplitude of both the reflected and transmitted wavefields. During acoustic FWI, the phase and amplitude difference due to mode conversion is unaccounted for and may lead to biased inversion results (Plessix and Krupovnickas, 2021).

In areas of the Southern North Sea, Cretaceous age chalk is found at very shallow depths and outcrops at the seafloor in places. Specifically, in the Breagh area discussed in this paper, chalk is present from the water bottom (50-80 m) down to a depth of 1.0 km and well data suggests it has a velocity around 4000 m/s. Beneath the chalk lie low velocity Jurassic sediments which generate Vp contrasts of up to ~2000 m/s. This forms a highly elastic boundary in the near surface – a feature likely to be pervasive across large parts of this region. This study area is covered by two narrow-azimuth, towed-streamer data sets with maximum offsets of 3 km and 6 km, respectively, acquired at ~90 degrees to each other. Several wells are also present in the area offering velocity and depth control in the shallow geology, as well as within deeper Permian evaporite units and hydrocarbon bearing Carboniferous sandstones. Previous studies have shown that acoustic FWI is unable to recover an accurate Vp model in shallow North Sea chalk environments due to strong elastic effects in the wavefield (Agudo et al., 2020), leading to those authors proposing complex workflows to remove the elastic effects from the recorded field data using matching filters. Similarities can also be drawn between the geology in this current study and that in other parts of the world, such as the Middle East (Leblanc et al., 2022; Adwani et al., 2022). In those areas the influence of elastic phenomena caused by alternating fast and slow layers in the near surface is shown to be non-trivial and acoustic approximations lead to erroneous velocity estimations in the shallow and at depth.

In this study we make initial comparisons between acoustic and elastic FWI (Masmoudi et al., 2023) in a shallow update down to 1.5 km. This update is mainly driven by the diving waves recorded in the data. Relative to the acoustic FWI, we find that the elastic FWI produces a better correlation of the inverted Vp with the sonic well-log data and subsequently propagates these shallow enhancements to the deeper section to provide improved image quality at the target level. This elastic FWI Vp model is then integrated into the general velocity model building workflow. Elastic FWI tests using reflection energy to 15 Hz extend a deeper update down to the target depth (~3 km). Comparing with the legacy model, the final result with elastic FWI shows imaging improvement in terms of reflector strength, event continuity and geological consistency at the target level.

Comparison of acoustic and elastic FWI updates to the shallow chalk

To assess the potential impact of the shallow chalk on FWI updates, we generated some modelled shot records (to 5 Hz) using the legacy model at locations where the chalk outcrops at the seafloor (Figure 1). The modelling was done using both acoustic and elastic wave equations, the latter utilising a Vs model derived from Vp by an empirical relation based on North Sea data. Figure 1c highlights how elastic modelling through the legacy model generates shots with transmitted arrivals more equivalent in appearance to the recorded data (Figure 1a), relative to the acoustic counterpart (Figure 1b). This is likely due to a better representation of how the energy of the wavefield partitions at the chalk interfaces,

especially the base chalk, and motivates the need for elastic FWI. The elastic wave propagation also models surface waves (Figure 1, blue arrows) similarly seen in the raw data but not present in the acoustic shots. Following this initial assessment, both acoustic and elastic FWI were run to 6.5 Hz, with the forward modelling comparison repeated with the respective acoustic and elastic FWI Vp model updates. Figure 1e demonstrates how the elastic FWI leads to good recovery of diving-wave energy at far offsets, as indicated by the dashed rectangles on this figure, in agreement with the real data (Figure 1a). The acoustic case (Figure 1d) also shows an improved data match over the legacy model (Figure 1b), but it is clearly struggling to reproduce the complexities in the recorded data via acoustic modelling/inversion, likely leading to a biased FWI result.

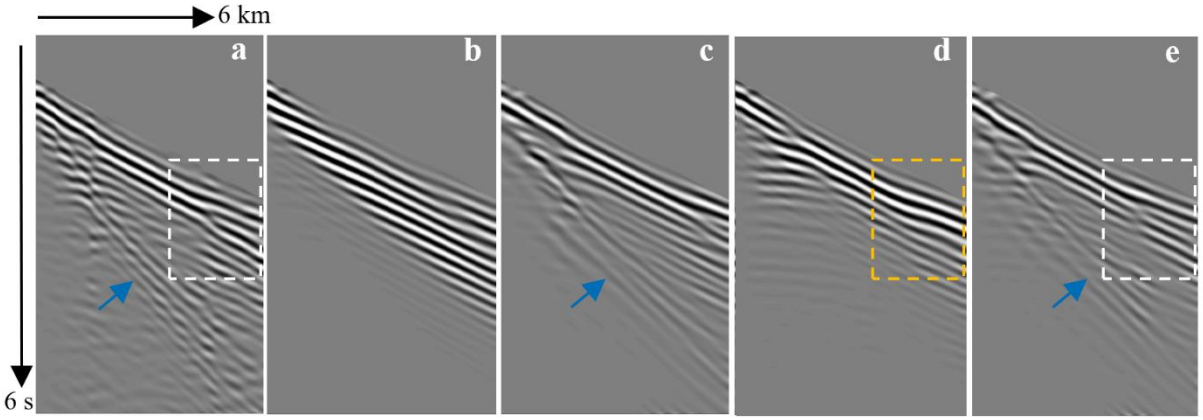

Figure 1 *Comparison of 5 Hz shot gathers over the shallow chalk area: (a) raw recorded data, (b) acoustically modelled data using legacy model, (c) elastically modelled data using legacy model, (d) acoustically modelled data using 6.5 Hz acoustic FWI updated model, and (e) elastically modelled data using 6.5 Hz elastic FWI updated model. Elastic modelling/inversion better represents the recorded data (white rectangles) compared with acoustic modelling (orange rectangle).*

Acoustic and elastic FWI were then run to 10 Hz down to a depth of 1.5 km. These updates were tapered into the legacy model and used to generate initial imaging comparisons, assessing the impact of the shallow update on the deeper image (Figure 2). The input Vp model was a smoothed version of the legacy Vp model for both updates. The elastic FWI preserves the fast velocities in the chalk layer and velocity inversion at the base chalk boundary (Figure 2e, yellow arrow). By comparison, the acoustic FWI reduces the velocity within the chalk and causes the velocities in the Jurassic to deviate from the sonic well-log data (orange arrows). This slow-down is also seen in Figure 2a where chalk velocities are generally decreased across the shallow section by acoustic FWI, whereas they remain sensible in elastic FWI (Figure 2b). Due to the complex geology, a multi-arrival, ray-based, controlled-beam migration (CBM) was used for the initial imaging assessment between the two FWI approaches. Relative to the acoustic FWI update (Figure 2c), migration with the elastic FWI update yields an improved structural image above the salt and at the Base Permian Unconformity (Figure 2d, green arrow). These imaging improvements can be related to the velocities in the chalk overburden and around a small, incised channel feature beneath the water bottom (blue arrow on Figure 2b).

Deeper salt updates with elastic FWI

After the initial shallow FWI update, the deeper model was refined through reflection tomography and some salt interpretation edits to mitigate the relatively shallow diving-wave penetration of the input data. While these traditional methods have their use, in this case they only captured a low frequency representation of the thin Zechstein carbonate and evaporite units. Figure 3a shows this limitation in the legacy model, which was built using well data and multiple passes of layer-based reflection tomography. Tests of a deeper 15 Hz elastic FWI update down to ~3 km (Figure 3c) demonstrates how the chalk improvements brought by the shallow pass of FWI are maintained, while also increasing the resolution of the velocity features at this higher frequency, such as the shallow channel (white arrows). Further, we see resolution of finer scale velocity structures within the salt, most notably the fast velocity,

basal anhydrite layer (black arrows). This fast velocity layer is also visible in the well data shown in Figures 3e and 3f, where we see an overall good correlation between the sonic log and elastic FWI update. Given that the recorded diving waves do not penetrate the deeper part of the model, this subsequent pass of elastic FWI is mainly driven by reflections. In this work, we utilised a time-lag cost function as this can provide a more robust inversion of reflections compared to the classical least-squares approach, as it minimises the risk of cycle skipping and better handles any remaining modelled and recorded data amplitude discrepancies (Wang et al., 2019). A 40 Hz reverse-time migration (RTM) is then used to honour the derived complexity in the updated model. Figures 3b and 3d, respectively, compare the RTM images of the legacy and elastic FWI updated model, where the new model clearly improves the reflector continuity and structural imaging (blue arrows). An equivalent acoustic FWI was also tested at this stage but again negatively impacted the chalk velocities.

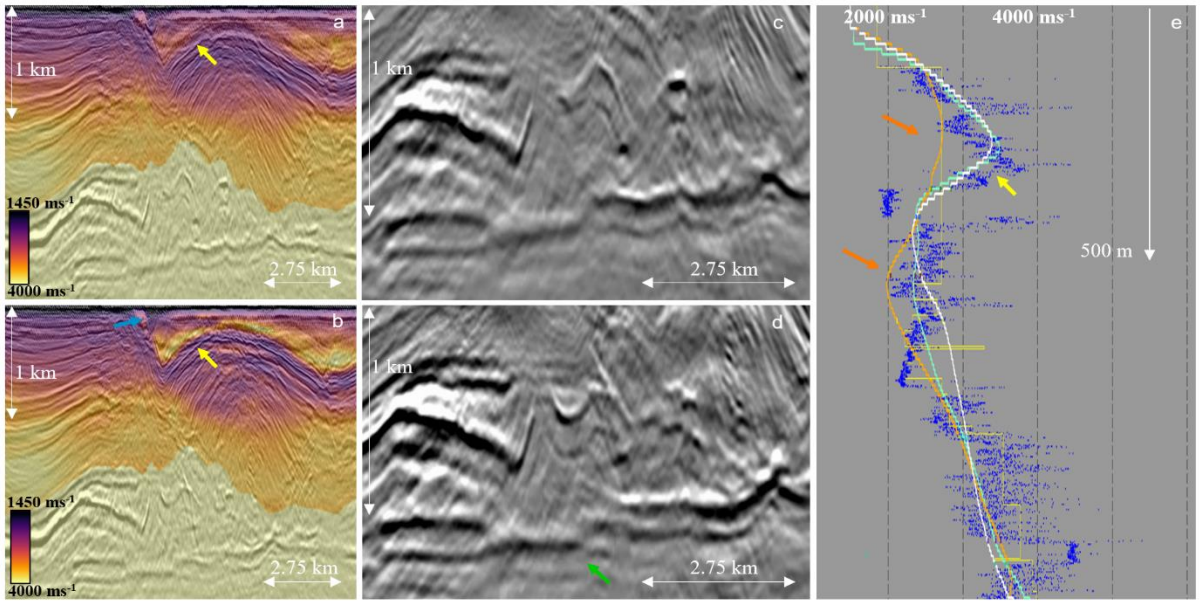

Figure 2 *Comparison of shallow 10 Hz acoustic and elastic FWI results (down to 1.5 km): (a) acoustic FWI updated model overlayed on corresponding migrated image, (b) elastic FWI updated model overlayed on corresponding migrated image, (c) CBM imaged with acoustic FWI model, (d) CBM imaged with elastic FWI model, and (e) shallow well data showing sonic log (blue), checkshot curve (yellow), input to FWI (white), acoustic FWI (orange) and elastic FWI (cyan).*

Conclusions

We have shown the potential of elastic FWI using short-offset, dual narrow-azimuth, towed-streamer data to yield improved velocity updates in shallow chalk regions of the Southern North Sea, where conventional tomography methods and acoustic FWI face shortcomings. Despite the limitations of streamer input data with short offsets and narrow azimuths, the elastic FWI led to an improved model showing strong alignment with well data and improved imaging over the legacy and acoustic FWI model at the target level.

Acknowledgements

We acknowledge TGS as data owner, together with INEOS Group Ltd as licensor of the data and sponsor of the reprocessing, for permission to show the real data. We also acknowledge INEOS Group Ltd (including Kevin Jaggs), ONE-Dyas and AMK Seismic, and thank CGG for permission to publish.

References

Adwani, A., Danilouchkine, M., Al-Siyabi, Q., Al-Droushi, O., Ten Kroode, F., Plessix, R-E. and Ernst, F. [2022] Onshore model building using elastic full-waveform inversion on surface and body waves: A case study from Sultanate of Oman. *Geophysics*, **87**, R413-R424.

Agudo, O.C., da Silva, N.V., Stronge, G. and Warner, M. [2020] Mitigating elastic effects in marine 3-D full-waveform inversion. *Geophys. J. Int.*, **220**, 2089-2104.
Leblanc, O., Sedova, A., Lambaré, G., Allemand, T., Hermant, O., Carotti, D., Donno, D. and Masmoudi, N. [2022] Elastic Land Full-Waveform Inversion in the Middle East: Method and Applications, *83rd EAGE Annual Conference & Exhibition*, Extended Abstracts, 1-5.
Masmoudi, N., Stone, W., Ratcliffe, A., Refaat, R. and Leblanc, O. [2022] Elastic Full-Waveform Inversion for Improved Salt Model Building in the Central North Sea. *83rd EAGE Conference & Exhibition Workshop Programme*, Extended Abstracts, 1-3.
Masmoudi, N., Stone, W. and Ratcliffe, A. [2023] Visco-elastic full-waveform inversion and imaging using ocean-bottom node data. *84th EAGE Conference & Exhibition*, Extended Abstracts, 1-5.
Plessix, R-E. and Krupovnickas, T. [2021] Low-frequency, long-offset elastic waveform inversion in the context of velocity model building. *The Leading Edge*, **40**, 342-347.
Wang, P., Zhang, Z., Mei, J., Lin, F. and Huang, R. [2019] Full-waveform inversion for salt: A coming of age. *The Leading Edge*, **38**, 204-213.
Wu, Z., Wei, Z., Zhang, Z., Mei, J., Huang, R. and Wang, P. [2022] Elastic FWI for large impedance contrast. *2nd International Meeting for Applied Geoscience & Energy*, SEG/AAPG, Expanded Abstracts, 3686-3690.
Zhang, Z., Wu, Z., Wei, Z., Mei, J., Huang, R. and Wang, P. [2020] FWI Imaging: Full-wavefield imaging through full-waveform inversion. *90th Annual International Meeting*, SEG, Expanded Abstracts, 656-660.

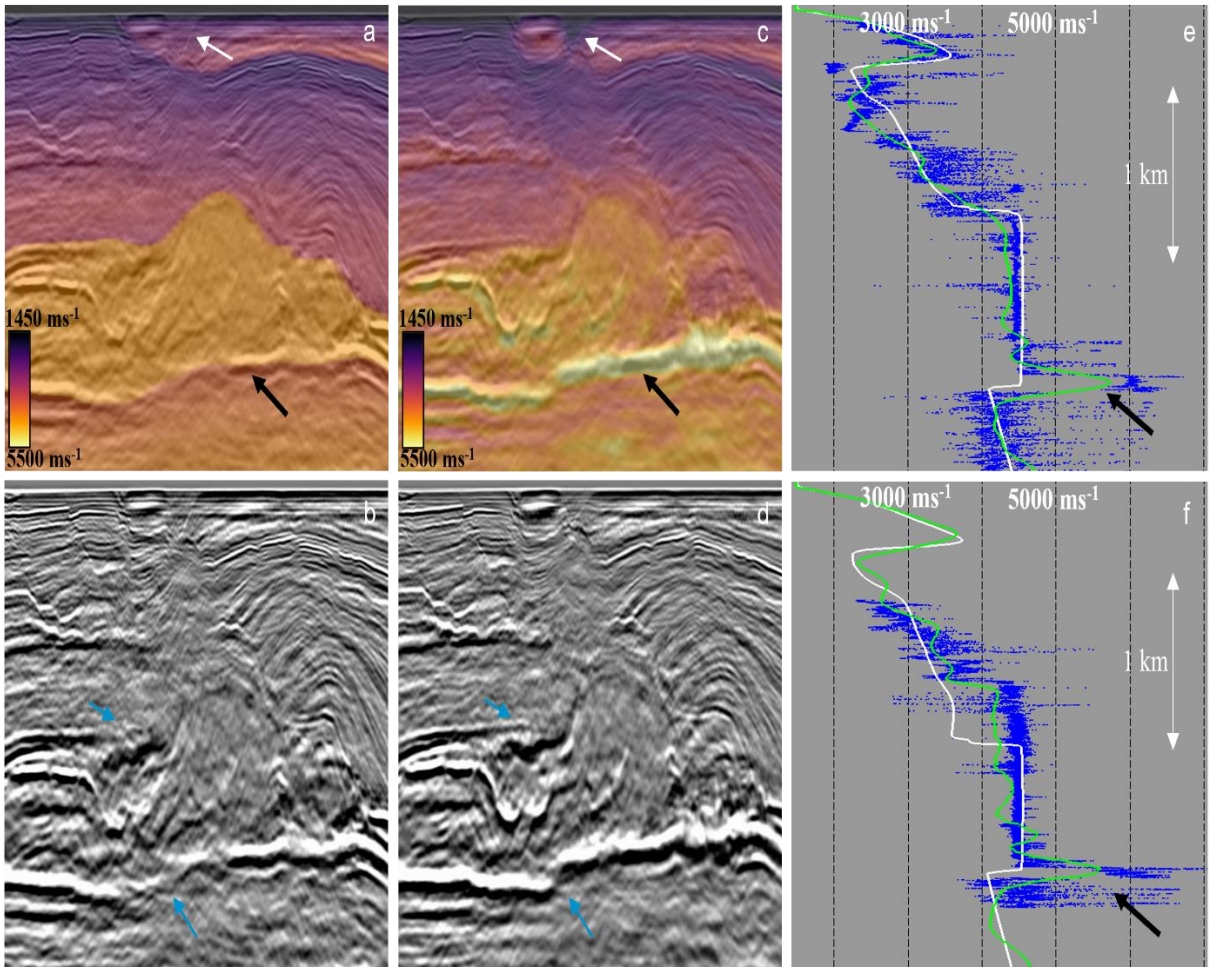

Figure 3 *40 Hz RTM comparison of legacy model with 15 Hz elastic FWI result: (a) legacy model overlayed on corresponding RTM image, (b) RTM image migrated with legacy model, (c) elastic FWI model overlayed on corresponding RTM image, (d) RTM image migrated with elastic FWI model. (e) and (f) show two well profiles with sonic log (blue), legacy model (white) and elastic FWI model (green).*